GEOPHYSICS, VOL. 56, NO. 4 (April 1991); P. 519–527, 8 FIGS.

Inverse *Q* filtering by Fourier transform

N. D. Hargreaves* and A. J. Calvert‡

ABSTRACT

Although some attention has been paid to the idea that seismic migration is equivalent to a type of deconvolution (of the spatial wavelet), less thought has been given to the opposite perspective: that deconvolution (of the earth Q filter) might itself be equivalent to a form of migration. The key point raised in this paper is that a dispersive 1-D backward propagation can form the basis of a number of different algorithms for inverse Q filtering, each of which is akin to a particular migration algorithm. An especially efficient algorithm can be derived by means of a coordinate transformation equivalent to that in the Stolt frequency-wavenumber migration.

This fast algorithm, valid for Q constant with depth, can be extended to accommodate depth-variable Q by cascading a series of constant Q compensations, as in cascaded migration. By combining a cascaded phase compensation with a windowed approach to amplitude compensation, we obtain an algorithm that is sufficiently efficient to be used routinely for prestack data processing. Data examples compare the results of conventional processing with the more stable phase treatment that can be obtained by including prestack inverse Q filtering in the processing.

INTRODUCTION

The attenuation of seismic energy by the earth, and the resulting nonstationarity of the recorded data trace, are fundamental issues in the wavelet processing of seismic data. Attenuation causes a loss of high-frequency energy with increasing traveltime and also a time-varying distortion of wavelet phase. Whereas any of a number of different data processing techniques can provide a reasonably adequate correction for seismic frequency loss (e.g., zero-phase deconvolution, time-variant spectral whitening), the time-varying phase distortion is often far more problematic. Wavelet phase, however, is what is of particular importance when the survey objective is the detailed analysis of stratigraphy, or if the processed data are to be input to inversion schemes that extract lithologic information.

In this paper we adopt a wave-propagation view of the earth Q filter and see inverse Q filtering as a process closely related to inverse wave propagation, or migration. We show that seismic data can be inverse Q filtered by backward propagating the data recorded at the surface, removing the interval effect of the Q filter as the wavefield is projected down through the earth. This approach can be used to derive a number of possible algorithms for inverse Q filtering, including one that is based on a coordinate transformation similar to that in the Stolt (1978) migration, and which has the computational efficiency of that approach. Given an assumed model of earth attenuation, this algorithm can efficiently correct for the time-variant phase distortion due to the earth filter.

Dispersion, the variation of seismic velocities with frequency, is a result of the requirement that wave propagation in an absorbing medium must be causal (Aki and Richards, 1980). The field and synthetic data examples in this paper were processed using the dispersion relationship derived by Futterman (1962) which is based on a "frequency-independent Q" model. The algorithm we derive is, however, not restricted to a specific model of Q dispersion, and other dispersion relationships such as those discussed by Azimi (1968) or Kjartannson (1979), could have been used.

Velocity dispersion, if it exists over the interval from seismic to sonic-logging frequencies, can produce time shifts which are important when seismic data are tied to sonic-log data. There is extensive literature on whether dispersion-generated drift between seismic and sonic-log data actually does occur, and prior to the mid-1970s the majority of authors concluded that the effect most likely did not exist; see for example O'Brien and Lucas (1971). Opinions have changed as sonic-logging technology has improved, and positive drift has been more consistently identified (see

Presented at the 57th Annual International Meeting, Society of Exploration Geophysicists. Manuscript received by the Editor June 6, 1989; revised manuscript received April 19, 1990.
*Western Geophysical, P.O. Box 18, 455 London Road, Isleworth, Middlesex TW7 5AB, UK.
‡Department of Geophysics and Astronomy, University of British Columbia, 129-2219 Main Mall, Vancouver, B.C., Canada V2T 1W5.
©1991 Society of Exploration Geophysicists. All rights reserved.

Goetz et al., 1979; Peyret and Mons, 1981; Stewart et al., 1984) and accepted as most likely caused by velocity dispersion due to attenuation.

A slight modification to our fast phase-compensation algorithm leads to a convenient way of trying synthetic seismograms and seismic data; the modified algorithm applies a time-variant stretch or compression to the data trace, without any other change to the amplitude or phase of the wavelet embedded in the data.

INVERSE Q FILTERING: A MIGRATION PERSPECTIVE

A seismic wave experiences a phase shift that depends upon both frequency and wavefront direction as it propagates through the earth; seismic migration is the process that corrects for the resultant mispositioning of events in the surface-recorded wavefield. In an earth where velocity varies only with depth, and if source and receiver are coincident, migration may be implemented by a phase shift of the data to backward propagate the surface wavefield into the earth, plus an imaging at each depth step (Gazdag, 1978). The backward propagation process may be written as

$$P(\Delta z) = P(0, k_z, \omega) \exp\left[-ik_z(k_x, \omega)2\Delta z\right], \quad (1)$$

where the wavefield P is expressed as a function of depth z and the transform variables k_x and ω. The downward continuation operator is given by the complex exponential; k_z is defined by the usual relation and depends upon the medium velocity $v(z)$:

$$k_z = \frac{\omega}{v(z)}\left[1 - \frac{v^2(z)k_x^2}{\omega^2}\right]^{1/2}. \quad (2)$$

Attenuation and dispersion are aspects of wave propagation that are usually neglected during migration, but which could also be treated by incorporating them into the downward continuation operator. For convenience and for quality control, however, we usually prefer to perform the correction for absorption and dispersion ("inverse Q filtering") separately from migration. Such a separation of the two processes cannot be exact, since in general the amount of inverse filtering needed depends upon both the path length and the wave direction if Q, the medium quality factor, varies with position. If, however, Q is constant with position, then the inverse filtering depends solely upon traveltime and not the wave direction, and an inverse Q-filter process can be separated from the migration. In this situation there is no distinction between prestack and poststack inverse Q filtering, since both the forward and the inverse filter depend solely on the traveltime of an event on the recorded trace, regardless of offset.

In a constant-Q earth, inverse Q filtering results from replacing expression (2) by

$$k_s = \frac{\omega}{v(s, \omega)} + \frac{i\omega}{2Q(\omega)v(s, \omega)}, \quad (3)$$

where s is distance along the raypath and $v(s, \omega)$ is now the frequency-dependent phase velocity.

Propagating a distance Δs along each of the raypaths from the shot and receiver toward a scatterer (prestack), and assuming that v is constant laterally over the raypath aperture, or propagating a one-way distance Δs along the two-way path to a scatterer (poststack), the wavefield P is given by

$$P(\Delta s, \omega) = P(0, \omega) \exp\left[\frac{-i\omega 2\Delta s}{v(s, \omega)}\right] \exp\left[\frac{\omega 2\Delta s}{2Q(\omega)v(s, \omega)}\right]. \quad (4)$$

The distance variable s can be converted to two-way traveltime τ by

$$\Delta\tau = \frac{2\Delta s}{v(s, \omega_{\text{ref}})},$$

where $v(s, \omega_{\text{ref}})$ is the velocity at an arbritrarily chosen reference frequency ω_{ref}, and expression (4) then becomes

$$P(\Delta\tau, \omega) = P(0, \omega) \exp\left[\frac{-i\omega v(s, \omega_{\text{ref}})\Delta\tau}{v(s, \omega)}\right] \times \exp\left[\frac{\omega v(s, \omega_{\text{ref}})}{2Q(\omega)v(s, \omega)}\right]. \quad (5)$$

The imaged and inverse Q-filtered wavefield $P(\tau, t = 0)$ is given by

$$P(\tau, t = 0) = \frac{1}{2\pi}\int P(\tau, \omega)\, d\omega. \quad (6)$$

After downward continuation to τ, an event generated by reflection at a travelpath distance s is at $t = 0$ and is there fully compensated for dispersive propagation and attenuation. The different frequency components of the event now all arrive at the same (common) time, rather than at the frequency-dependent arrival times of the surface-recorded data. In a retarded timeframe $t' = t + \tau$ the event would be at a time governed by its travelpath length and by the velocity at the reference frequency; the downward continuation would have replaced the dispersive medium velocity with the reference velocity constant with frequency.

Repeated solution of equations (5) and (6), stepping down in $\Delta\tau$ and computing $P(\tau, t = 0)$ at each depth step, gives an inverse Q-filter algorithm akin to phase-shift migration; a time-domain version of the algorithm would be similar to a finite-difference migration.

In a manner analogous to Stolt (1978), however, we can make the following change of variable in equation (5):

$$\omega' = \omega \frac{v(s, \omega_{\text{ref}})}{v(s, \omega)}. \quad (7)$$

[Since Q has been assumed to be independent of position, ω' is also independent of position if the ratio $v(s, \omega_{\text{ref}})/v(s, \omega)$ depends only on Q, as in the Futterman (1962) or the Kjartansson (1979) dispersion relationships.]

Equations (5) and (6) can then be combined to give

$$P(\tau, t = 0) = \frac{1}{2\pi}\int P[0, \omega(\omega')]\frac{d\omega}{d\omega'} \times \exp\left[-i\omega'\tau\right] \exp\left[\frac{\omega'\tau}{2Q}\right] d\omega'. \quad (8)$$

If we neglect the amplitude effect of Q, equation (8) is an inverse Fourier transform in the new frequency variable ω' and can be solved by the fast Fourier transform. $d\omega/d\omega'$ is the Jacobian of the transformation from ω to ω' and is computed from the velocity dispersion relationship. Steps in the solution of equation (8) are: (i) forward Fourier transform the surface recorded trace; (ii) scale by $d\omega/d\omega'$ and interpolate to evenly spaced values of ω'; and (iii) inverse Fourier transform the interpolated data. The computational cost of this procedure has been found to be similar to that of the Weiner-Levinson deconvolution.

The coordinate transformation of equation (7) is essentially the same as that used in the frequency shift-and-scale approach of Robinson (1979). In the time domain, dispersion is a frequency-dependent time scaling; in the frequency domain this becomes a frequency and amplitude scaling of the transform values. The transformation is applied by a frequency-domain interpolation, using sinc or other interpolation operators [hence the title of Robinson's (1982) paper: "Time-variable dispersion processing through the use of phased sinc functions"].

Similar algorithms for removing dispersion have been derived by other authors. Booer et al. (1977) and Beresford-Smith and Mason (1980) used a related algorithm for pulse compression, the latter in the context of dispersive guided waves in coal seams. Beresford-Smith and Rango (1988) used the technique to remove dispersive near-surface noise from data recorded in Arctic regions.

We can obtain some physical insight into the nature of the algorithm by considering how the phase spectrum of an arrival in a dispersive medium is mapped to that which would be observed in a nondispersive medium. In Figure 1 we apply the coordinate transformation of equation (7) to the phase curves of two events with different traveltimes. The nonlinear phase response of the dispersive medium is converted to the linear phase spectrum that would have been obtained if the medium velocity had been constant and equal to the velocity at the reference frequency. The events have different travelpath lengths and different phase curves, but the dispersive and nondispersive curves for each intersect at the reference frequency. The coordinate transformation simultaneously straightens both dispersive phase curves regardless of their traveltime. Each reflection becomes a symmetric zero-phase event centered at a time determined by its travelpath length and the velocity at the reference frequency.

Cascaded inverse Q filtering

A depth-variable Q structure in a horizontally stratified earth can be inverse Q filtered by a series of constant-Q compensations (as in cascaded migration; Larner and Beasley, 1987).

Bickel et al. (1985) give a general expression for the effective Q value at a traveltime τ in a depth-variable medium; in the case of a two-layered model, reduces to

$$\frac{\tau}{Q} = \frac{\tau_1}{Q_1} + \frac{\tau - \tau_1}{Q_2}, \tag{9}$$

where Q_1 is the Q value of the first layer, τ_1 is the traveltime to the boundary between the two layers (with τ_1 less than τ), and Q_2 is the Q value of the second layer. Rewriting this expression as

$$\frac{\tau}{Q} = \frac{\tau}{Q_1} + (\tau - \tau_1)\left(\frac{1}{Q_2} - \frac{1}{Q_1}\right) \tag{10}$$

shows that the forward Q filtering experienced by an event at time τ is equivalent to a combination of forward filtering with a Q value of Q_1 from time zero to time τ, plus forward filtering by $(1/Q_2 - 1/Q_1)^{-1}$ from time τ_1 to time τ. The data at time τ can therefore be inverse filtered by two passes of depth-constant Q inverse Q filtering, the first using a Q value of Q_1 applied to data starting at time zero, the second using a Q value of $(1/Q_2 - 1/Q_1)^{-1}$ applied to data starting at τ.

This two-pass approach can be extended to an arbitrary number of depth layers, and is analogous to the cascaded migration approach of Larner and Beasley (1987), in which a depth-variable velocity structure is migrated by means of a cascaded series of (nearly) constant-velocity migrations.

Cascaded inverse Q filtering as described here is valid for horizontal Q layering and reflections of zero dip. We would expect to be able to use the technique in practice in areas of low dips and small lateral variations in Q, a restriction similar to that in time migration. Also, for prestack data, the start times of each stage of the cascade need to be adjusted

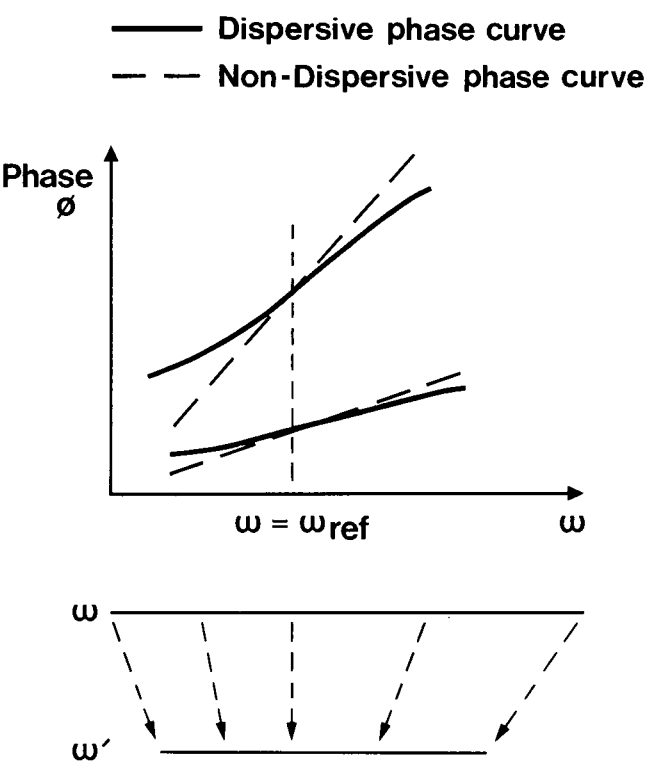

FIG. 1. Inverse Q filtering by frequency scaling. The fast phase-compensation algorithm converts the curved line phase responses of the dispersive medium to the straight-line responses of the nondispersive medium by means of a coordinate transformation from ω to ω'. This simultaneously straightens all the dispersive phase curves from different events, regardless of their traveltime.

as appropriate to the nonzero offset traveltimes at each offset.

Figure 2 is an example of cascaded phase-only inverse Q filtering [using the Futterman (1962) dispersion relationship] applied to a portion of synthetic data. The first stage of the cascade uses a Q value equal to Q_1, the Q value of the first layer; after this stage the data are fully compensated down to the bottom of that layer but are only partially compensated below that point. The second stage of the cascade starts at the bottom of the first layer and uses a Q value of $(1/Q_2 - 1/Q_1)^{-1}$, completing the compensation down to the bottom of the second layer. After this stage events in the third layer in this example are overcompensated, and the final stage of the cascade must proceed by forward rather than inverse Q filtering. This stage uses a Q value of $(1/Q_3 - 1/Q_2)^{-1}$, which is negative; the fast algorithm performs either forward or inverse Q filtering, depending upon the sign of the Q value supplied to it, in much the same way that the Stolt (1978) frequency-wavenumber domain migration can perform either migration or modeling.

Tying sonic and seismic data

When a raw sonic log is calibrated using check shots, the objective is to convert depths on the sonic-log data to seismic traveltimes; the calibration accommodates the dispersion-generated drift, in addition to correcting for any other sources of timing mismatch. However, check shots may often be unreliable, and seismic and sonic events may still not tie after calibration. If Q values are available and if the mis-tie is in fact due to dispersion and not some other source of error, then a modified version of our algorithm can provide an alternative way of tying the times of seismic data and raw uncalibrated sonic data.

Our fast phase-compensation algorithm uses a frequency-domain coordinate transformation to adjust the arrival time of different frequencies to the arrival time of the reference frequency for the phase compensation. An alternative way of expressing the coordinate transformation is

$$\frac{\omega'}{\omega} = \frac{v(\omega_{\text{ref}})}{v(\omega)} = \frac{v(\omega_{\text{ref}})}{2s}\,\frac{2s}{v(\omega)} = \frac{\tau}{\tau_{\text{ref}}}, \tag{11}$$

where s is the path length, τ is the arrival time of frequency ω, and τ_{ref} is the arrival time of the reference frequency ω_{ref}. This form of the transformation indicates that it changes the arrival time of each frequency ω, with velocity $v(\omega)$, to the arrival time of the reference frequency ω_{ref}.

A closely related transformation is

$$\frac{\omega'}{\omega} = \frac{\tau_1}{\tau_2} = \frac{v(\omega_2)}{v(\omega_1)}. \tag{12}$$

This transformation changes the arrival times of all the frequencies of an event by the same ratio, as if the velocity of the event were changed from $v(\omega_1)$ to $v(\omega_2)$. This is a time-varying stretch or compression of the data trace with no other change in the relative phases of each component; it can be implemented by a relatively minor modification to the algorithm discussed previously based on equation (8).

If ω_1 is chosen equal to the center frequency of the seismic passband and ω_2 to the sonic-logging frequency, the effect of the transformation is to move events from the seismic arrival times to sonic-log traveltimes, subtracting the dispersion-induced drift. Choosing ω_1 equal to the sonic-logging frequency and ω_2 equal to the central seismic frequency corrects sonic-log data to seismic traveltimes. (Figure 6 shows how this approach can be used to improve the time tie between a raw, uncalibrated, sonic log derived synthetic and a portion of processed seismic data.)

GAIN-LIMITED AMPLITUDE COMPENSATION

Although both amplitude and phase inverse Q filtering can be accomplished by the 1-D phase-shift algorithm of equations (5) and (6), the "Stolt-like" algorithm of equations (7) and (8) is restricted to phase-only inverse Q filtering. However, an adequate amount of wavelet compression can generally be obtained by a windowed amplitude treatment, in which deterministic inverse filters are applied to a small number of windows of data. Far fewer windows (perhaps five or six at the most) can be used for the amplitude treatment than might be needed for a windowed phase treatment.

To avoid overamplification of data noise, the amplitude treatment must be restricted to the range of frequencies over which the signal, in some sense, dominates the noise. This can be done by cutting off the action of the operators at a constant limiting gain value, so that the active frequency range of the operators varies with time in a way that parallels the change of signal bandwidth along the trace.

Figure 3 shows the result of applying a gain-limited amplitude compensation of this sort to a portion of noisy synthetic data. After the amplitude compensation, the data are still nonstationary because of the time-varying change of bandwidth of the amplitude compensation operators; this is an unfortunate but unavoidable consequence of the presence of data noise, which progressively encroaches on the usable signal spectrum as time increases. This change of bandwidth with time also has implications for the relative amplitude behavior of the data, and in the absence of other effects the wavelet peak amplitudes decrease with increasing time, as a result of the decrease of bandwidth with increasing time.

DATA EXAMPLES

North Sea marine data example

The data examples in Figures 4 through 6 are from the central-Graben High area of the North Sea, to the south of the Erskine complex. The target in this area is a Jurassic sand-shale sequence truncated by the late Cimmerian unconformity, which is the event at approximately 3.2 seconds on the right of Figure 4.

The wavelet processing applied to generate the unmigrated stack section in Figure 4 consisted of (1) a deterministic deconvolution that shaped the far-field air-gun source signature to its minimum-phase equivalent; (2) a windowed prestack spiking deconvolution; (3) a combination of time-variant spectral whitening and phase-conversion poststack that was equivalent to a windowed poststack spiking deconvolution.

In Figure 5, the wavelet processing consisted of signature deconvolution with the desired output wavelet a zero-phase

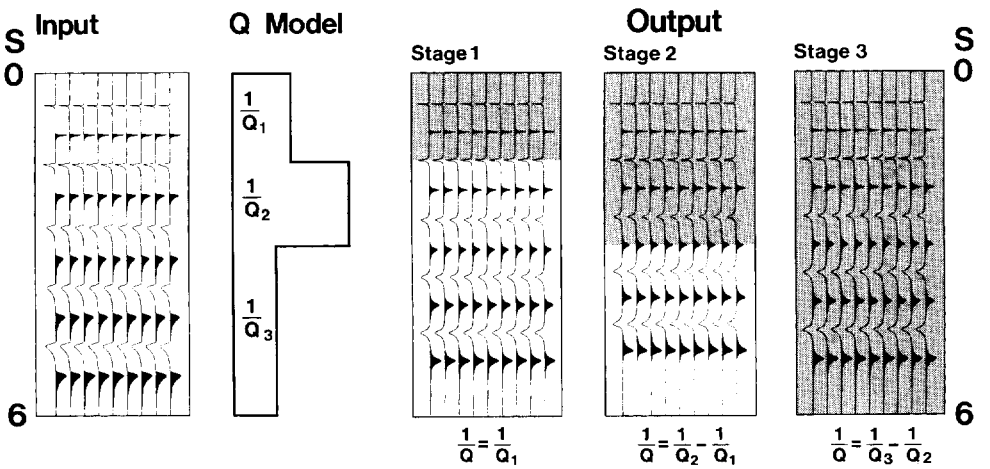

FIG. 2. Cascaded inverse Q filtering. A depth-variable Q structure can be treated by a series of depth-constant Q compensations in a manner equivalent to cascaded migration. In the figure, Q phase compensation has been applied to the input synthetic data set by means of a three-stage cascade of the fast constant-Q algorithm.

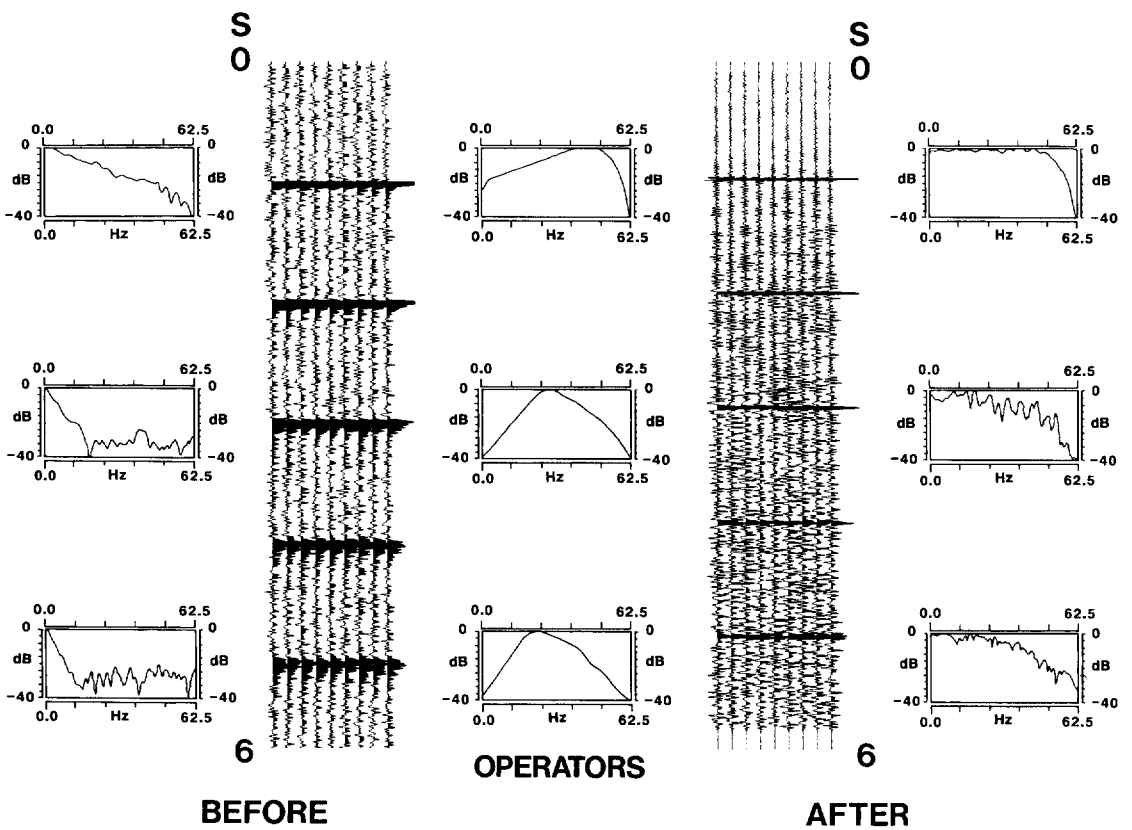

FIG. 3. Gain-limited amplitude compensation. Amplitude compensation of these synthetic data (together with phase compensation by a cascaded phase-only inverse Q filter) has been performed by applying deterministic inverse filters to a small number of windows of data; to prevent the data noise from being overamplified, the amplitude spectra of the operators, shown in the center of the figure, were clipped at a user-determined maximum gain level. The signal bandwidth of the noisy forward Q-filtered synthetic on the left is progressively reduced at late times; the amplification of high frequencies in the inverse Q-filtered result on the right of the figure has been limited to approximately the range of signal frequencies over which the signal energy dominates the noise.

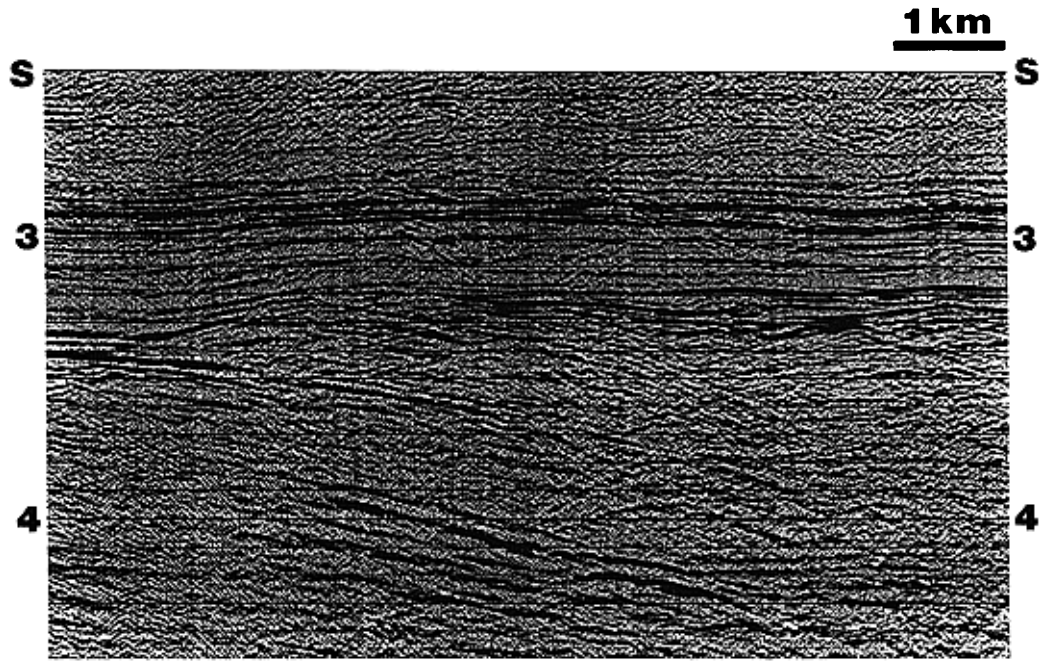

FIG. 4. Portion of North Sea stack data treated by prestack and poststack windowed spiking deconvolution.

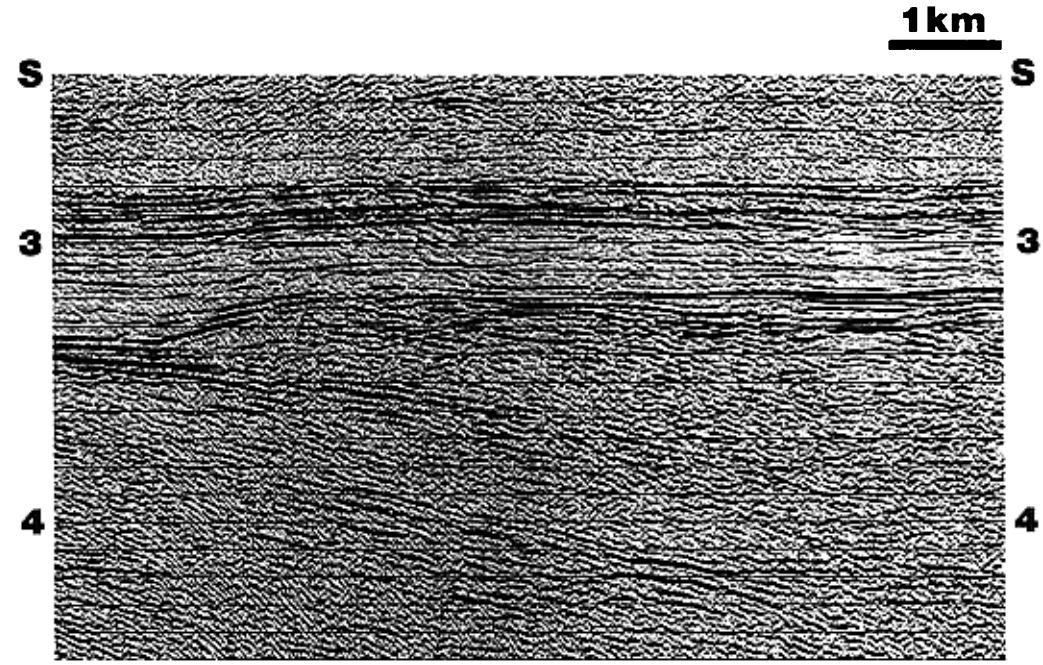

FIG. 5. The same data as in Figure 4, treated instead by prestack inverse-Q amplitude- and phase filtering, together with a windowed, gapped deconvolution prestack. No further wavelet processing was applied after the stack. The target horizon at 3.2 s in Figures 4 and 5 exhibits dissimilarities in several places due to the different phase action of the two processing schemes. Features in the inverse Q-filtered section are more likely to be geologically significant because the phase treatment of the inverse Q filter is more stable.

equivalent of the air-gun signature; prestack inverse Q amplitude and phase filtering using Q values derived from spectral analysis of the prestack data; and a two-window, prestack gapped deconvolution. The inverse Q filtering was performed using a cascaded version of the fast phase-compensation algorithm, together with a gain-limited, windowed amplitude compensation. The reference frequency for the inverse Q filtering in this example (and in the subsequent data examples) was chosen to be in the center of the seismic passband to leave events positioned close to original seismic traveltimes. No further wavelet processing was applied after the stack; all other processing applied to these two sections was identical.

Both processing sequences flatten the amplitude spectrum of the data to approximately the same extent, although the deterministic amplitude treatment of the inverse Q filter may have recovered slightly more high frequencies in Figure 5 than does the statistical deconvolution of Figure 4. The amplitude and phase corrections obtained from the statistical deconvolution depend upon the noise in the window of data from which it is derived and on the uniformity of the reflections within that window. Both these factors may vary across the section, so that by incorporating inverse Q filtering into the processing sequence we can expect to obtain a more stable treatment than by means of the statistical deconvolution alone. The target horizon at 3.2 s in Figures 4 and 5 exhibits dissimilarities in several places due to the different phase action of the two methods, and one can have greater confidence that the features seen in Figure 5 are geologically significant because of the stability of the inverse Q filter.

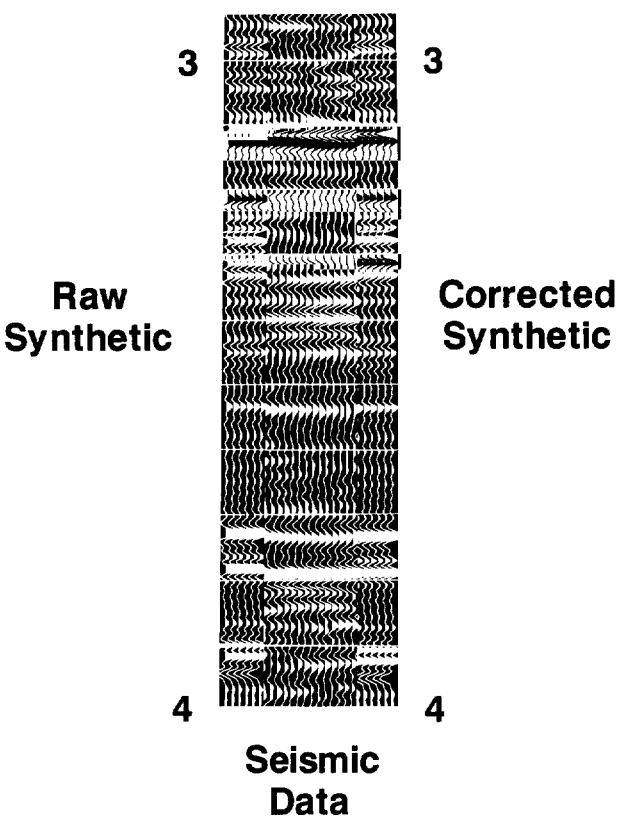

FIG. 6. Well-log synthetic data before and after correction for dispersion-induced well-log drift. After correction for drift using the Q values derived from spectral decay analysis of the prestack seismic data, the times of the seismic and the corrected synthetic reflections have a better match.

A published sonic log from a well close to a line in this area was used to generate the reflection synthetic shown on the left of Figure 6. This uncalibrated synthetic has events positioned according to integrated sonic-log traveltimes, and the dispersion-induced drift between the sonic-derived reflections and the equivalent events in the seismic data can clearly be seen at later reflection times in the figure. The synthetic can be adjusted for the drift using the Q values obtained from spectral analysis of the seismic data, and after the drift adjustment has been added to the synthetic the seismic and synthetic data match. This result confirms the relationship between the amplitude and phase actions of the earth filter; a Q function estimated from the amplitude spectrum of the seismic data can be used to match the traveltimes of the seismic and sonic-log data.

Middle East land data example

Figures 7 and 8 show the result of applying two alternative processing sequences to vibrator data from the Middle East (courtesy of ADNOC, Abu Dhabi). The section in Figure 7 had a windowed spiking deconvolution applied before the stack and a phase compensation of the vibrator wavelet after the stack (to correct for the minimum-phase action of the deconvolution on the vibrator wavelet). The section in Figure 8 had inverse Q amplitude and phase filtering applied before the stack, using a Q value of 100 obtained from spectral decay analysis, followed by prestack deconvolution with a 24 ms gapped operator. No further processing was applied to this section, and all other processing applied to each of the two sections was identical.

The principal issues in the interpretation of these data are recognition of the Upper Cretaceous reefal buildup in the shallower part of the section above the prominent marker horizon, and detailed analysis of the underlying prospective evaporite and clastic carbonate reservoir sequence. The arrows indicate some of the places the conventionally processed data exhibit significant differences from the inverse Q-filtered section. The lateral variability of the wavelet here suggests a lack of phase control and implies that the deconvolution may have encountered difficulties because of noise. The more consistent, deterministic, phase treatment of the inverse Q-filtered data is likely to be important, for example, for interpretation of the reefal buildup marked by the circle in the figures.

CONCLUSION

In this paper we develop an efficient frequency-domain method for inverse Q filtering that treats the time variance of the phase of the seismic wavelet, given an assumed model for the velocity dispersion that accompanies attenuation. Our approach is based on the understanding that attenuation and dispersion are aspects of wave propagation, and that inverse Q filtering can be accomplished as an integral part of seismic migration or, more conveniently, as a single-channel process closely related to migration.

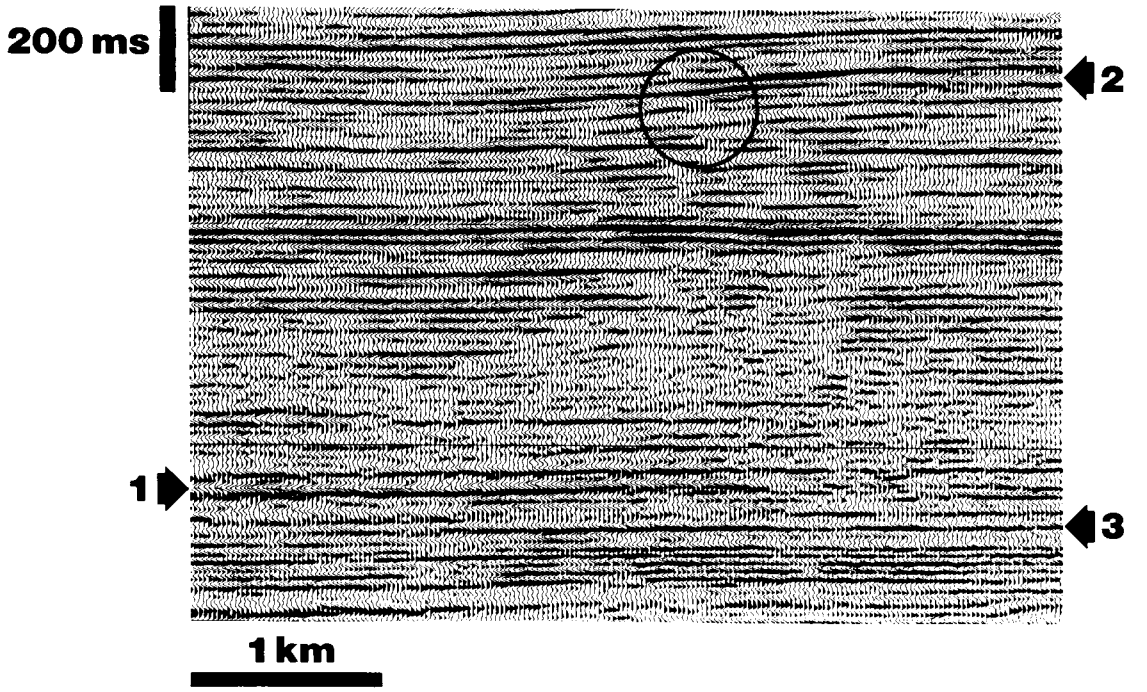

FIG. 7. Portion of vibrator data from the Middle East (courtesy of ADNOC, Abu Dhabi) treated by windowed spiking deconvolution before stacking.

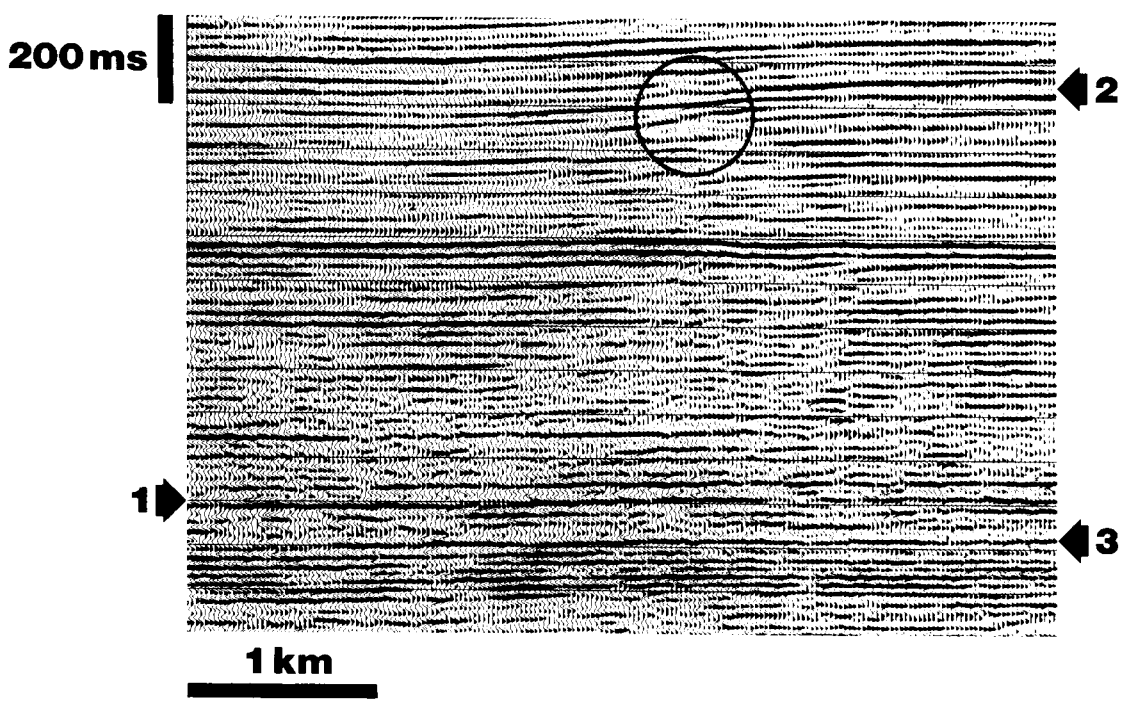

FIG. 8. The same data set as in Figure 7, but with inverse Q amplitude and phase filtering applied before the stack, together with a prestack gapped, rather than spiking, deconvolution. The arrows and circle indicate areas in which the inverse Q-filtered section exhibits a possibly more stable phase treatment than do the conventionally processed data.

The fast, "Stolt-like" algorithm we derive is restricted to phase-only inverse Q filtering and must be combined with a windowing approach for the treatment of the wavelet amplitude spectrum. The amplitude operators we use are designed to be active only up to a maximum gain level to avoid overamplifying noise outside the signal passband. Although the signal spectrum is flattened within the passband, the processed data remain nonstationary, which is an aspect of the process that must be accepted as an unavoidable consequence of the existence of data noise. It is the gain limitation, as much as the efficiency of the phase compensation, that makes it possible to use the process routinely in prestack data processing.

ACKNOWLEDGMENTS

Thanks to Keith Hirsche for his insights into the dispersive nature of the Q filter; Ken Larner for his thoughts on cascaded inverse Q filtering and his help and support throughout this project; Dave Caliga and Dave Nichols for their professional programming assistance; Steve Blight and Yvonne Cummerson for the graphic artwork.

REFERENCES

Aki, K., and Richards, P. G., 1980, Quantitative seismology, theory and methods, 1: W. H. Freeman.

Azimi, S. A., Kalinin, A. V., Kalinin, V. V., and Pivovarov, B. L., 1968, Impulse and transient characteristics of media with linear and quadratic absorption laws: Phys. Solid Earth, 88–93.

Beresford-Smith, G., and Mason, I. M., 1980, A parametric approach to the compression of seismic signal by frequency transformation: Geophys. Prosp., **28**, 551–571.

Beresford-Smith, G., and Rango, R. N., 1988, Dispersive noise removal in $t - x$ space: Application to Arctic data: Geophysics, **53**, 346–358.

Bickel, S. H., and Natarajan, R. R., 1985, Plane-wave Q deconvolution: Geophysics, **50**, 1426–1439.

Booer, A. K., Chambers, J., and Mason, I. M., 1977, Fast numerical algorithm for the recompression of dispersed time signals: Electron. Lett., **13**, 453–455.

Futterman, W. I., 1962, Dispersive body waves: J. Geophysics Res., **67**, 5729–5291.

Gazdag, J., 1978, Wave-equation migration with the phase-shift method: Geophysics, **43**, 1342–1355.

Goetz, J. F., Dupal, L., and Bowles, J., 1979, An investigation into discrepancies between sonic logs and checkshot velocities: APEA J., **19**, 131–141.

Kjartansson, E., 1979, Constant Q-wave propagation and attenuation: J. Geophys. Res., **84**, 4737–4748.

Larner, K., and Beasley, C., 1987, Cascaded migration: Improving the accuracy of finite-difference migration: Geophysics, **52**, 618–643.

O'Brien, P. N. S., and Lucas, A. L., 1971, Velocity dispersion of seismic waves: Geophys. Prosp., **19**, 1–26.

Peyret, O., and Mons, F., 1981, Sonic versus seismic velocities; positive drift study; recording frequency effect: Schlumberger technical memorandum M-083210.

Robinson, J. C., 1979, A technique for the continous representation of dispersion in seismic data: Geophysics, **44**, 1345–1351.

——— 1982, Time-variable dispersion processing through the use of "phased" sinc functions: Geophysics, **47**, 1106–1110.

Stewart, R. R., Huddleston, P. D., and Kan, T. K., 1984, Seismic versus sonic velocity; a vertical seismic profile study: Geophysics, **49**, 1153–1168.

Stolt, R., 1978, Migration by Fourier transform: Geophysics, **43**, 23–48.